View metadata, citation and similar papers at core.ac.uk

brought to you by CORE

provided by Elsevier - Publisher Connector

Fungal Genetics and Biology 48 (2011) 1027–1033

Contents lists available at SciVerse ScienceDirect

Fungal Genetics and Biology

journal homepage: www.elsevier.com/locate/yfgbi

The metalloreductase FreB is involved in adaptation of *Aspergillus fumigatus* to iron starvation

Michael Blatzer [a], Ulrike Binder [b], Hubertus Haas [a,*]

[a] Division of Molecular Biology/Biocenter, Fritz-Pregl-Str. 3, Innsbruck Medical University, A-6020 Innsbruck, Austria
[b] Section for Hygiene and Medical Microbiology, Fritz-Pregl-Str. 3, Innsbruck Medical University, A-6020 Innsbruck, Austria

ARTICLE INFO

Article history:
Received 24 March 2011
Accepted 26 July 2011
Available online 5 August 2011

Keywords:
Iron
Copper
Reductive iron assimilation
Siderophore
Ferrireductase

ABSTRACT

Aspergillus fumigatus employs two high affinity iron uptake mechanisms, siderophore mediated iron uptake and reductive iron assimilation (RIA). The *A. fumigatus* genome encodes 15 putative metalloreductases (MR) but the ferrireductases involved in RIA remained elusive so far. Expression of the MR FreB was found to be transcriptionally repressed by iron via SreA, a repressor of iron acquisition during iron sufficiency, indicating a role in iron metabolism. FreB-inactivation by gene deletion was phenotypically largely inconspicuous unless combined with inactivation of the siderophore system, which then decreased growth rate, surface ferrireductase activity and oxidative stress resistance during iron starvation. This study also revealed that loss of copper-independent siderophore-mediated iron uptake increases sensitivity of *A. fumigatus* to copper starvation due to copper-dependence of RIA.

© 2011 Elsevier Inc. Open access under CC BY-NC-ND license.

1. Introduction

Iron is an indispensable trace element for all eukaryotes and almost all prokaryotes. As a transition element iron can adopt two ionic forms, the reduced ferrous (Fe^{2+}) and the oxidized ferric (Fe^{3+}) state. The capacity to accept or donate electrons makes iron the major redox mediator in biology. Either alone or incorporated into iron–sulfur clusters or heme, iron is required for fundamental cellular processes like the tricarboxylic cycle, oxidative stress detoxification as well as biosynthesis of amino acids, desoxyribonucleotides, and sterols. However, iron excess has the ability to generate toxic reactive species that can damage cellular components (Halliwell and Gutteridge, 1984). Despite its high abundance in the Earth' crust, the bioavailability of iron is very limited owing to its oxidation into insoluble Fe^{3+}-hydroxides by atmospheric oxygen. Consequently, all organisms have developed tightly regulated mechanisms in order to balance uptake, storage and consumption of iron.

Aspergillus fumigatus is a typical ubiquitous saprophytic mold. Nevertheless, it causes life-threatening invasive diseases especially in immuno-compromised patients and has become the most common airborne fungal pathogen of humans (Tekaia and Latge, 2005). *A. fumigatus* employs two high-affinity iron uptake systems, siderophore-assisted iron uptake and reductive iron assimilation (RIA), both of which are induced upon iron starvation (Schrettl et al., 2004, 2007, 2008). Siderophores are low molecular mass, Fe^{3+}-specific chelators (Haas et al., 2008, 2003). *A. fumigatus* excretes the siderophores fusarinine C and triacetylfusarinine C (TAFC) to mobilize extracellular iron. Subsequent to chelation of iron, the Fe^{3+}-forms of fusarinine C and TAFC are incorporated by specific transporters, e.g. MirB (Haas et al., 2003). *A. fumigatus* possesses also intracellular siderophores, hyphal ferricrocin and conidial hydroxyferricrocin, for distribution and storage of iron (Schrettl et al., 2007; Wallner et al., 2009). RIA starts with reduction of Fe^{3+}-sources to the more soluble Fe^{2+} by plasma membrane-localized ferrireductases, which have not been identified in *A. fumigatus* yet (Kosman, 2010). Subsequently, Fe^{2+} is re-oxidized and imported by a protein complex consisting of the ferroxidase FetC and the iron permease FtrA. Ferroxidases belong to the multicopper oxidase family resulting in copper-dependence of RIA (Hassett et al., 1998; Kosman, 2010). Moreover, *A. fumigatus* employs low affinity iron uptake, which has not been characterized at the molecular level (Schrettl et al., 2004).

Both extra- and intracellular siderophores contribute to pathogenic growth because elimination of the entire siderophore system (Δ*sidA* mutant) results in absolute avirulence of *A. fumigatus* in a murine model of invasive pulmonary aspergillosis, while deficiency in either extracellular (Δ*sidF* or Δ*sidD* mutants) or intracellular siderophores (Δ*sidC* mutants) causes partial attenuation of virulence (Schrettl et al., 2004, 2007). Genetic inactivation of RIA (Δ*ftrA* mutant) does not affect virulence of *A. fumigatus* (Schrettl et al., 2004, 2007). Nevertheless, several lines of evidence indicate

Abbreviations: RIA, reductive iron assimilation; MR, metalloreductase; TAFC, triacetylfusarinine C; NOX, NADPH oxidase; IMR, integral membrane reductase; AMM, Aspergillus minimal medium.

* Corresponding author. Fax: +43 512 9003 73100.
E-mail address: hubertus.haas@i-med.ac.at (H. Haas).

1087-1845 © 2011 Elsevier Inc. Open access under CC BY-NC-ND license.
doi:10.1016/j.fgb.2011.07.009

that RIA also plays a role during infection: (i) elimination of extracellular siderophores causes only partial attenuation of virulence, (ii) genome-wide expression profiling revealed induction of both the siderophore system and RIA during initiation of murine infection, and (iii) mutants lacking both RIA and the siderophore system (Δ*ftrA*Δ*sidA* double mutant) are unable to grow unless supplemented with siderophores or extremely high iron concentrations fueling low-affinity iron uptake (McDonagh et al., 2008; Schrettl et al., 2004, 2007). Of note, RIA has been shown to be crucial for virulence in animal models of the siderophore-lacking species *Candida albicans* and *Cryptococcus neoformans* and the siderophore-producing species *Rhizopus oryzae* (Eichhorn et al., 2006; Ibrahim et al., 2010; Jung et al., 2008; Ramanan and Wang, 2000). Moreover, RIA is essential for virulence of the plant-pathogenic siderophore-producing species *Ustilago maydis* (Eichhorn et al., 2006; Jung et al., 2008; Ramanan and Wang, 2000).

Metalloreductases (MR) belong to the integral membrane reductases (IMR) protein family (Grissa et al., 2010). IMR are present in all fungal species and can be classified into at least 24 subgroups. IMR are homologous to fungal NADPH oxidases (NOX), which reduce oxygen to superoxide (O_2^-) for antimicrobial defense (e.g. mammalian gp91phox) or signaling (Aguirre et al., 2005; Frey et al., 2009). IMR activity requires NADPH, FMN, and heme. Like NOX, IMRs oxidize cytoplasmic NADPH and transfer the electron across the plasma membrane to reduce small molecules, dioxygen in the case of NOX (yielding thus the superoxide anion) and mostly metals (Fe^{3+} and/or Cu^{2+}) in the case of IMRs. Fungal MR have so far been biochemically or genetically characterized exclusively in three yeast species, the *Saccharomycotina* species *Saccharomyces cerevisiae* and *C. albicans* as well as the *Taphrinomycotina* species *Schizosaccharomyces pombe* (Kosman, 2003).

The *A. fumigatus* genome encodes 15 putative MR (Nierman et al., 2005). Combining phylogenetic analysis, genome-wide expression profiling, gene deletion analysis with subsequent phenotyping and biochemical analysis demonstrated that the MR encoded by AFUA_1G17270, termed FreB, is involved in adaptation to iron starvation and functions most likely in RIA.

2. Materials and methods

2.1. Fungal strains and growth conditions

The fungal strains used are listed in Table 1. All strains used in this study were grown at 37 °C in *Aspergillus* minimal medium (AMM) according to Pontecorvo et al. (1953) containing 1% glucose as carbon source and 20 mM glutamine as nitrogen source. For iron-replete (+Fe) conditions, $FeCl_3$ was added to a final concentration of 30 μM, copper-replete (+Cu) conditions contained 16 μM $CuSO_4$. For iron (−Fe) and copper (−Cu) starvation, addition of iron and copper, respectively was omitted. Liquid cultures were conducted in 0.5 l Erlenmeyer flasks inoculated with 10^8 conidia and shaken with 200 rpm at 37 °C. The iron chelator bathophenantroline disulfonate (BPS) was used in a final concentration 0.2 mM for plate assays.

Table 1
A. fumigatus strains used in this study.

Strain	Genotype	Reference
Wild type (wt)	ATCC46645	American type culture collection
Δ*sidA*	ATCC46645; *sidA::hph*	Schrettl et al. (2004)
Δ*sreA*	ATCC46645; *sreA::hph*	Schrettl et al. (2008)
Δ*freB*	ATCC46645; *freB::ptrA*	This work
Δ*freB*Δ*sidA*	ΔsidA; *freB::ptrA*	This work
freB^{C}Δ*sidA*	Δ*sidA*; Δ*freB*, *freB*, *ble*	This work

2.2. Manipulation of nucleic acids and strain construction

In order to delete the *freB* gene in ATCC46645 (wt) and Δ*sidA* strains (Schrettl et al., 2004), the bipartite marker technique was used (Nielsen et al., 2006). Therefore, fungal strains were co-transformed with two DNA fragments, each containing overlapping, but incomplete fragments of the pyrithiamine resistance-conferring *ptrA* gene fused to the *freB* 5′- and 3′-flanking sequences. The *freB* 5′-flanking region (1.1 kb) was PCR-amplified from genomic DNA using primers oFreb1 and oFreB3r, with an added *Hind*III restriction site. For the amplification of the 3′-flanking region (0.9 kb) primers oFreB4 and oFreB6r were employed. Following gel-purification, the 5′- and 3′-flanking regions were digested with *Hind*III and *Pst*I, respectively. The *ptrA* cassette was released from plasmid pSK275 by digestion with *Hind*III and *Pst*I (2.0 kb) and subsequently ligated to the 5′- and 3′-flanking regions, respectively. The transformation constructs A and B containing fusions of overlapping *ptrA* cassette fragments with the *freB* 5′- and 3′-flanking regions, respectively, were PCR amplified from the ligation products using primer pairs oFreB2/oPtrA1 (2.2 kb) and oFreB5r/ptrA2 (2.3 kb). For transformation of fungal strains, both constructs A and B were simultaneously used (Kubodera et al., 2000). Due to the use of nested primers and restriction enzyme digestions, the final length of the *freB* 5′- and 3′-flanking regions was 1.0 kb and 0.8 kb, respectively. This strategy deleted the region +230 to +2356 according to the translation start site (Fig. S1).

For reconstitution of *freB* in Δ*freB*Δ*sidA*, a 5.6 kb PCR-fragment generated with primers oFreB7 and oFreB5r was used in co-transformation with the plasmid pAN8.1 carrying the phleomycine resistance cassette (Punt and van den Hondel, 1992).

Transformation was carried out as described previously (Schrettl et al., 2007). For selection of transformants, 0.1 μg ml^{-1} pyrithiamine (Sigma) or 0.04 μg ml^{-1} phleomycine were used. Screening of transformants was performed by PCR and confirmed with Southern blot analysis. The hybridization probes for Southern blot analysis of Δ*freB* and *freB*^{c} strains were generated by PCR using the primers oFreB 1 and oFreB3r and oPtrA1 and otrA2, respectively (Fig. S1 and Table S1).

2.3. Northern blot analysis and nucleic acid manipulations

RNA was isolated using TRI reagent (Sigma). For Northern analysis, 10 μg of total RNA were analyzed as described previously. Hybridization probes and primers are listed in Table S1. For extraction of genomic DNA, mycelia were homogenized and DNA was isolated according to Sambrook et al. (1992).

2.4. Analysis of siderophores

Analysis of siderophores was carried out by reversed phase HPLC as described previously (Oberegger et al., 2001). Moreover, to quantify extracellular or intracellular siderophores, culture supernatants or cellular extracts were saturated with $FeSO_4$ and siderophores were extracted with 0.2 volumes of phenol. The phenol phase was separated and subsequent to addition of five volumes of diethylether and 1 volume of water, the siderophore concentration of the aqueous phase was measured photometrically using a molar extinction factor of 2996/440 nm (M^{-1} cm^{-1}).

2.5. Ferrireductase assay

Ferrireductase activity was measured as described previously by Nyhus et al. (1997). The assay relies on the formation of a red BPS–Fe^{2+} ($\varepsilon_{535\ nm}$ = 22.14 M^{-1} cm^{-1}) from colorless HEDTA–Fe^{3+}. The assay contained in a total volume of 2.0 ml, 1.0 ml of fungal culture including mycelia and culture, 1.0 mM BPS, and 1.0 mM

Fe^{3+}HEDTA. Formation of BPS–Fe^{2+} was measured after incubation for 1 h at 37 °C in the dark and mycelia were separated by centrifugation prior to reading the absorbance. BPS–Fe^{2+} produced in the same time frame by the culture supernatant (e.g. due to production of extracellular reductants) was subtracted.

2.6. Phylogenetic analysis

Putative MR were identified in fungal genomes by TBLASTN and psiBLAST searches (Altschul et al., 1997). The identified protein sequences were used for a clustalW alignment with the Pasteur bioweb.2 database (http://mobyle.pasteur.fr). Based on this alignment a rooted tree was generated using the Pasteur bioweb.2 database (Neron et al., 2009).

2.7. Oxidative stress sensitivity assay

Susceptibility to reactive oxygen species was determined as described previously (Sugareva et al., 2006). 10^7 *A. fumigatus* conidia were mixed with 10 ml −Fe-AMM top agar and poured onto −Fe-AMM plates. In the middle of the plate a hole of 5 mm in diameter was pricked out and filled with 100 µl of a 100 mM H_2O_2 solution. The diameter of the growth inhibition zone was measured after incubation for 24 h at 37 °C.

2.8. Measurement of intracellular reactive oxygen species

100 µl −Fe-AMM and +Fe-AMM, respectively, were inoculated with 3×10^3 conidia in 96 well plates. After 18 h of incubation at 37 °C, H_2O_2 was added to a final concentration of 2.0 mM; in control experiments, H_2O_2 treatment was omitted. After incubation for 30 min, 6-carboxy-2′,7′-dichlorofluorescin diacetate (DCF-DH) was added and fluorescence was recorded after incubation for another 30 min using a fluorescence microplate reader (Bertold Mithras LB940) with excitation at 485 nm and emission at 535 nm (Wang and Joseph, 1999). The fluorescence was measured for hydrogen-peroxide treated and non-treated samples and normalized to that of the non-treated wt.

2.9. Statistical analysis

Results were presented as mean ± standard deviation and statistical significance was defined by *t*-test with *p*-values < 0.05 and <0.01, respectively.

3. Results and discussion

3.1. A. fumigatus encodes 15 putative MR

MR contain a ferrireductase-like transmembrane motif (CDD:174502; 273-390) and a NOX-Duox-like FAD/NADP-motif (CDD:99783; 451.741). BLASTP and TBLASTN homology searches identified 15 putative MR-encoding genes in the *A. fumigatus* genome and 10 in the genome of *Aspergillus nidulans* (Galagan et al., 2005; Nierman et al., 2005), a close *A. fumigatus*-relative, which however lacks homologs to FtrA and FetC and consequently RIA (Eisendle et al., 2003; Haas et al., 2008). The numbers of putative MR encoded by the genomes of different fungal species are quite different, e.g., nine in *S. cerevisiae*,. sixteen in *C. albicans*, two in *S. pombe*, six in *U. maydis*, and six in *C. neoformans*. MR functions have been analyzed in most detail in *S. cerevisiae* (Philpott and Protchenko, 2008; Rees and Thiele, 2007; Singh et al., 2007); its nine putative MR are termed Fre1-8 and YGL160W. Fre1-4 are involved in RIA. Fre1 and Fre2 comprise the majority of surface reductase activity; they are required for growth on media that contain low concentrations of Fe^{3+}-salts, and can catalyze the reductive release of iron from a variety of siderophores. Because Fe^{2+} has a low affinity for siderophore ligands, reduction of siderophore-bound Fe^{3+} results in the release of Fe^{2+}, which can be taken up by the Fe^{2+}-specific transporters. Fre3 and Fre4 can catalyze the reductive uptake of iron bound to hydroxamate siderophores and rhodotorulic acid, respectively. Fre1p and Fre2p are also copper reductases, converting Cu^{2+} to usable Cu^{1+} (Georgatsou et al., 1997). Fre6 localizes to the vacuolar membrane, where it functions in the reductive transport of iron and copper from the vacuole to the cytosol. The functions of the other *S. cerevisiae* MR are unknown. Expression of the genes encoding Fre1-6 is induced during iron starvation. The gene encoding Fre1 is additionally and that encoding Fre7 exclusively induced by copper starvation. *S. pombe* possesses two putative MR, of which one, termed Frp1, is transcriptionally repressed by iron and essential for RIA (Roman et al., 1993). The *C. albicans* genes encoding the MR Cfl1 and Cfl95 are repressed by iron and can restore reductase activity to the orthologous *S. cerevisiae* mutant (Hammacott et al., 2000; Knight et al., 2002, 2005). Furthermore, the transcript levels of the *C. albicans* genes encoding the MR Frp1 and Fre2 are upregulated by alkaline growth conditions and Frp1 is induced additionally by iron starvation (Baek et al., 2008). Additionally, iron repression has been reported for the genes encoding the following fungal MR: *A. nidulans* FreA, *C. neoformans* Fre1, *U. maydis* Fer9.

Phylogenetic analyses of the MR of these five ascomycetous and two basidiomycetous species revealed that the iron-repressed MR of *S. cerevisiae* (Fre1-6) and 11 of the 16 MR of *C. albicans* are inparalogs, i.e. they evolved in *Saccharomycotina* after the split from the other subpyhla (Fig. 1). Moreover, the MR from different species with proven function in RIA (*S. cerevisiae* Fre1-5 and *S. pombe* Frp1) or showing upregulation during iron starvation (*C. neoformans* Fre1 and *A. nidulans* FreA) are only distantly related. These data indicate that prediction of a function in RIA solely based on evolutionary relation is impossible.

3.2. Expression of freB is repressed by iron in a SreA-mediated way

Genome wide transcriptional profiling indicated SreA-dependent down-regulation of the putative *A. fumigatus* MR-encoding gene AFUA_1G17270, termed *freB*, in a shift from iron depleted to iron-replete conditions (Schrettl et al., 2008). SreA is a transcriptional repressor of genes involved in both siderophore-mediated iron uptake and RIA during iron-replete conditions. Northern blot analysis confirmed SreA-dependent repression by iron of *freB* similar to the known SreA target *mirB* (Fig. 2A), which encodes a siderophore transporter (Haas et al., 2008). In contrast to many other SreA target genes, however, *freB* is not genomically clustered with other iron-regulated genes (Schrettl et al., 2008). In contrast to iron starvation, copper starvation did not upregulate the *freB* transcript level (Fig. 2A), which makes a role in copper metabolism rather unlikely. Together with several known genes involved in high-affinity iron uptake, *freB* was previously found to be upregulated during initiation of infection in a murine model of invasive pulmonary aspergillosis, which stresses its role in iron metabolism in vivo (McDonagh et al., 2008).

3.3. FreB is involved in adaptation to iron starvation and the siderophore system increases copper starvation resistance

To functionally characterize the *freB* gene product, the FreB-coding region was replaced by the pyrithiamine resistance marker gene *ptrA* in *A. fumigatus* wild type strain ATCC46645 (wt) and the descending Δ*sidA* mutant strain, which lacks siderophore biosynthesis, as described in 2.1, Table 1 and Fig. S1. The resulting gene deletion strains were termed Δ*freB* and Δ*freB*Δ*sidA*, respectively.

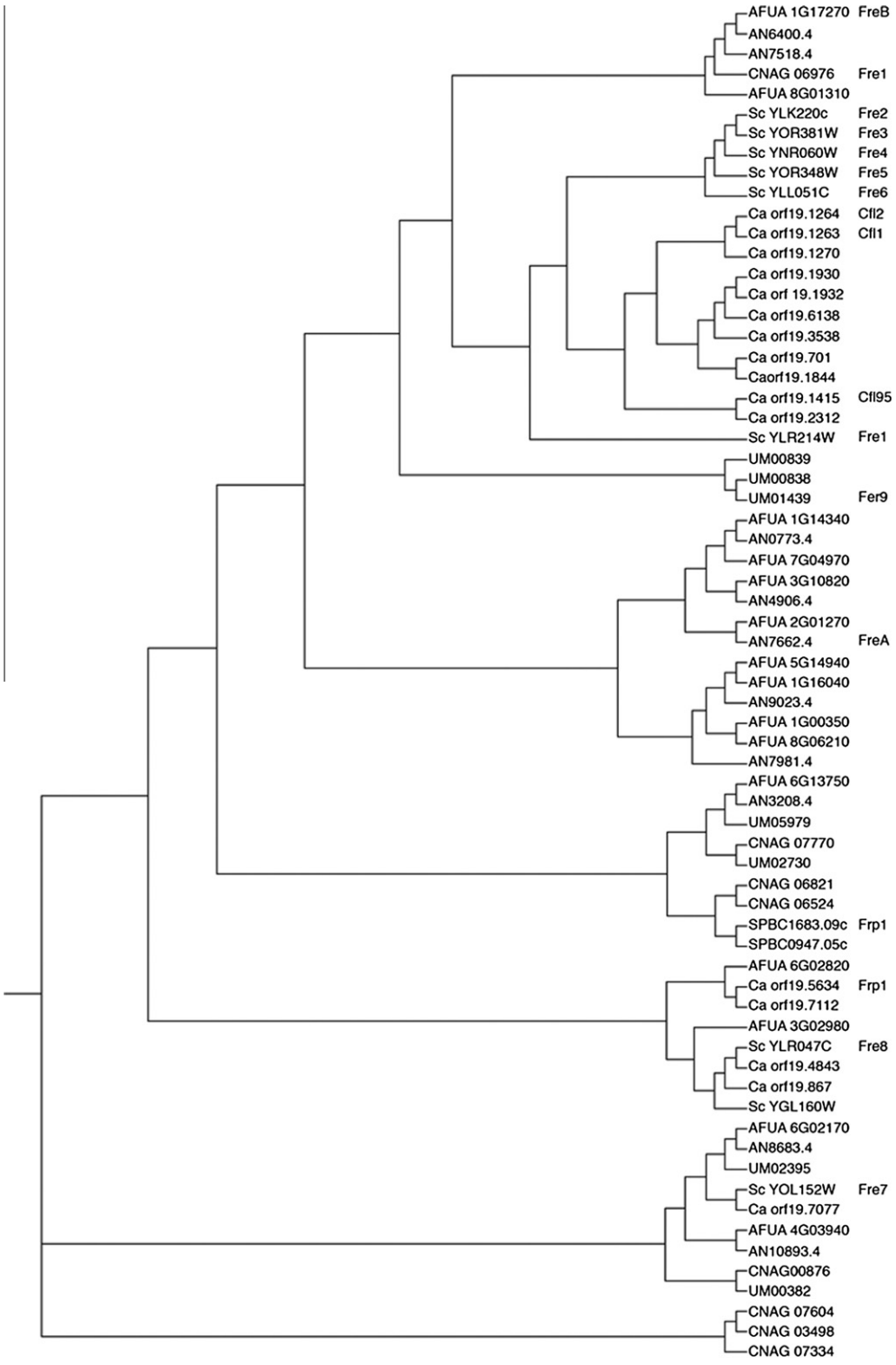

Fig. 1. Phylogentic analysis (rooted neighbor joining tree) of MR from 5 asomycetous and two basidiomycetous species. For MR previously analyzed functionally or transcriptionally (see Section 3.1) the protein names are given. Abbreviations are the following: AFUA. *A. fumigatus*; AN. *A. nidulans*; Ca. *C. albicans*; CNAG. *C. neoformans*; Sc. *S. cerevisiae*; SPBC. *S. pombe*; UM. *U. maydis*.

To ensure characterization of gene deletion-specific effects, a single functional copy of *freB* was homologously integrated at the *freB* locus in Δ*sidA*Δ*freB*, yielding *freB*^{c}Δ*sidA*. In all tests performed, *freB*^{c}Δ*sidA* behaved as Δ*sidA* (Table 2 and data not shown). Deletion of *freB* in Δ*sidA* was carried out to block possible compensation of FreB-deficiency by the siderophore system, as we found previously that inactivation of RIA does not lead to growth defects unless carried out in a Δ*sidA* background (Schrettl et al., 2004).

Based on the similarity of FreB with MR, we compared the biomass production of the wt and mutant strains in response to iron and copper availability in submersed liquid cultures (Table 2). Biomass production of Δ*freB* resembled that of the wt during iron and

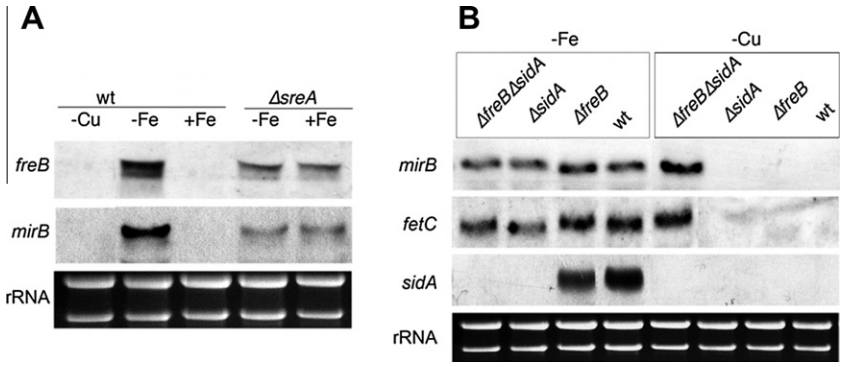

Fig. 2. Expression of *freB* is repressed by iron via SreA but not by copper (A) and copper starvation transcriptionally upregulates high-affinity iron uptake in Δ*freB*Δ*sidA* (B). For Northern analysis *A. fumigatus* strains were grown for 24 h in liquid flask cultures under iron/copper-replete (++), iron depleted (−Fe), and copper depleted (−Cu) conditions. The SreA target genes *sidA*, *mirB*, and *fetC* encode the siderophore-biosynthetic ornithine monooxygenase, a siderophore transporter, and the RIA component ferroxidase, respectively (Haas et al., 2008). Ethidium bromide-stained rRNA is shown as control for loading and quality of RNA.

Table 2
FreB-deficiency decreases liquid growth rate during iron starvation (−Fe) but not copper starvation (−Cu). Biomass production was normalized to that of the wt under the respective growth conditions. The biomass production of the wt was 1150.4 ± 27.6, 873.2 ± 14.8, and 499.1 ± 13 mg in +Fe + Cu (30 μM Fe and 16 μM Cu), −Cu, and −Fe, respectively. The given values are the mean ± STD of four biological replicates. Statistical significance was analyzed by *t*-test ($^{*}p < 0.05$; $^{**}p < 0.01$) comparing Δ*sidA* and Δ*freB* with wt but Δ*freB*Δ*sidA* and *freB*^{c}Δ*sidA* with Δ*sidA*.

	−Fe	−Cu	+Fe + Cu
Δ*freB*	92.6 ± 2.4**	98.0 ± 1.7**	101.7 ± 2.9
Δ*sidA*	80.9 ± 2.7**	75.6 ± 1.6**	90.7 ± 3.4*
Δ*freB*Δ*sidA*	37.0 ± 1.7**	70.0 ± 0.9**	86.0 ± 2.3**
freB^{c}Δ*sidA*	73.7 ± 2.5	73.9 ± 0.7	91.6 ± 2.1

copper sufficiency (+Fe + Cu) and copper starvation (−Cu) but was 7.4% decreased during iron starvation (−Fe). Deficiency in siderophore-mediated iron uptake by SidA-deficiency impaired the biomass production to a higher degree during copper starvation (−24.4%) than during iron starvation (−19.1%). The increased sensitivity of Δ*sidA* to copper starvation is most likely explained by the fact that iron supply of this mutant relies solely on RIA, which is copper dependent. In contrast, the wt can alternatively acquire iron via the copper-independent siderophore system. Compared to Δ*sidA*, FreB-deficiency in Δ*sidA* had only a mild effect during iron and copper sufficiency (−4.7%) as well as copper starvation (−5.6%) but biomass production was reduced by 43.9% during iron starvation. These data indicate that FreB is crucial mainly for adaptation to iron starvation but plays no significant role during copper starvation, which is consistent with the *freB* expression pattern (see Fig. 2A). The subtle phenotype of Δ*freB* compared to Δ*freB* Δ*sidA* indicates that FreB-deficiency can be compensated by the siderophore system. The latter is underlined by a 23% increase of TAFC production by Δ*freB* compared to wt after 24 h of submersed growth during iron starvation (data not shown). Previously, compensatory upregulation of TAFC production was observed to be caused also by a lack of the RIA component FtrA (Schrettl et al., 2004), which implicates FreB function in RIA as well.

Assaying radial growth rate with classical plate tests (Fig. 3A), i.e. starting from point-inoculated 10^4 conidia, SidA-deficiency was found to drastically decrease radial growth during starvation for either iron or copper, which again demonstrates that the siderophore system confers resistance against starvation for iron and copper as seen in liquid cultures (see Table 2). FreB-deficiency did impact the growth pattern in neither wt nor Δ*sidA* backgrounds (Fig. 3A). In plate growth assays starting from single conidia (Fig. 3B), SidA-deficiency was also found to drastically decrease the colony size unless supplemented with high iron concentrations (hFe, 1.5 mM). FreB-deficiency did not influence radial growth in the wt background but blocked colony formation in the Δ*sidA* background during iron starvation (−Fe).

To further analyze the link between iron and copper metabolism, expression of components of the two high-affinity iron uptake systems was analyzed at the transcriptional level in wt, Δ*freB*, Δ*sidA*, and Δ*freB*Δ*sidA* (Fig. 2B). Iron starvation, but not copper starvation, upregulated the transcript levels of *sidA*, *mirB* and the ferroxidase-encoding *fetC*, which is involved in RIA (Schrettl et al., 2004), in wt and Δ*freB*. Δ*sidA* displayed a similar expression pattern but lacked *sidA* transcripts due to the deletion of this gene. In contrast to Δ*sidA*, *mirB* and *fetC* transcript levels were upregulated in Δ*freB*Δ*sidA* not only by iron starvation but also copper starvation. The most likely explanation is that the copper requirement of this mutant is increased and affects iron acquisition due to impaired siderophore-mediated iron uptake and hampered RIA due to FreB-deficiency.

Taken together, these data underline a crucial role of FreB in adaptation to iron starvation and reveal that the siderophore system increases resistance against copper starvation. Moreover, the different growth assays displayed varying sensitivity in detection of defects in adaptation to iron starvation.

3.4. FreB-deficiency reduces ferrireductase activity

Iron-replete liquid cultures of the wt lacked measurable surface ferrireductase activity (data not shown). In contrast, iron starvation induced ferrireductase activity in the wt indicating iron-regulation at transcriptional or enzymatic level (Fig. 4A). Δ*sidA* displayed a 3.6-fold higher ferrireductase activity probably to compensate the loss of siderophore-mediated iron uptake. FreB-deficiency decreased the ferrireductase activity by 33% in wt and 73% Δ*sidA* backgrounds. These data demonstrate that FreB accounts for a significant part of the ferrireductase activity in wt and the major ferrireductase activity in the absence of the siderophore system.

3.5. FreB-deficiency increases sensitivity to hydrogen peroxide

Plate diffusion assays revealed that deficiency in either FreB or SidA slightly increases sensitivity to hydrogen peroxide. Simultaneous deficiency in both FreB and SidA resulted in substantial increased sensitivity to hydrogen peroxide (Fig. 4B). These data underline that the two high-affinity iron acquisition systems, siderophore-mediated iron uptake and RIA, are mutually able to partially compensate the individual inactivation.

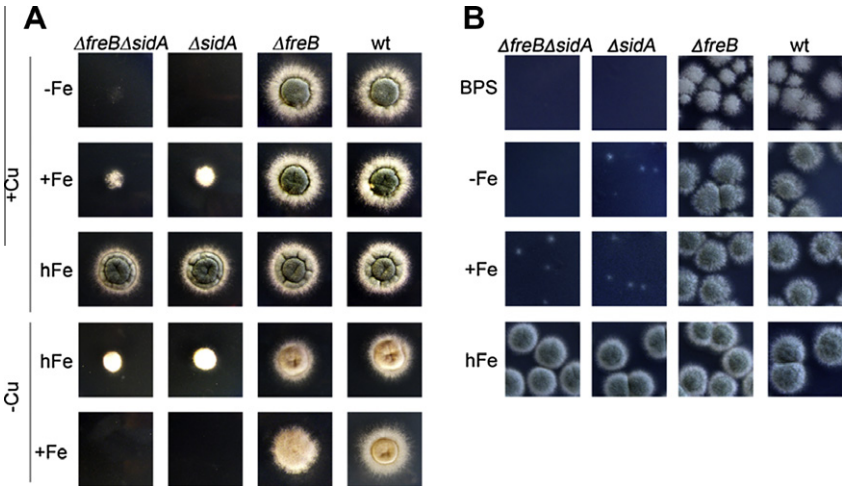

Fig. 3. SidA-deficiency results in sensitivity to starvation for copper and iron, respectively, (A) and FreB-deficiency results in the inability of colony formation from single conidia during iron starvation (B). (A) 10^4 conidia of the respective strain were point-inoculated on AMM plates containing the different iron or copper concentrations (+Fe, 30 μM; hFe, 1.5 mM; + Cu, 16 μM) and were incubated for 48 h at 37 °C. (B) About 20 conidia were plated on copper-replete media containing the indicated iron concentration. BPS inhibits strains lacking the siderophore system by blocking of RIA (Schrettl et al., 2004). Copper starvation blocks formation of the green conidial pigmentation resulting in yellow pigmentation.

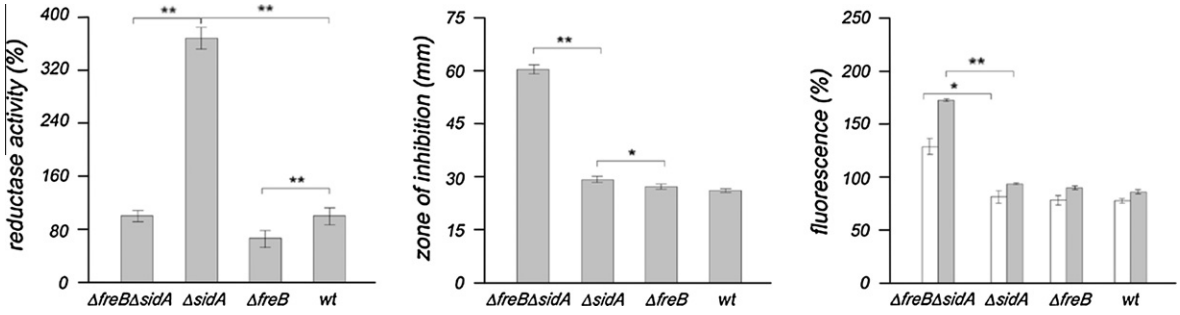

Fig. 4. FreB-deficiency reduces ferrireductase activity (A), increases sensitivity to hydrogen peroxide (B), and increases cellular reactive oxygen species in particular in the absence of siderophore biosynthesis (Δ*freB*Δ*sidA*). Ferrireductase activity was measured after 24 h of submersed growth at 37 °C during iron starvation and normalized to that of the wt. Hydrogen peroxide sensitivity was analyzed after 48 h of growth in plate diffusion assays. The level of cellular reactive oxygen species was quantified without (open bars) and with (grey bars) hydrogen peroxide treatment by the dichlorofluorescein assay, in which fluorescence is proportional to the level of reactive oxygen species. The given values are the mean ± STD of three biological replicates. Statistical significance was analyzed as described in Table 2 ($^*p < 0.05$; $^{**}p < 0.01$).

To alternatively quantify the cellular oxidative stress, the dichlorofluorescein assay (Wang and Joseph, 1999), which measures the oxidation of non-fluorescent dichlorofluorescin derivates into fluorescent dichlorofluorescein derivates by reactive oxygen species, was applied. In this assay, the emitted fluorescence is directly proportional to the cellular level of reactive oxygen species. Compared to Δ*sidA*, the fluorescence of the Δ*freB*Δ*sidA* was increased 1.5-fold and after hydrogen peroxide treatment even 1.8-fold (Fig. 4C). Compared to wt, the Δ*freB* and Δ*sidA* strains displayed only a mild, statistically insignificant, increase in fluorescence. These data are in good agreement with the hydrogen peroxide resistance of the strains.

The increase in both oxidative stress and sensitive to hydrogen peroxide of Δ*freB*Δ*sidA* is most likely due to the decreased iron supply, which deranges cellular metabolism and in particular impairs iron-dependent enzymes involved in detoxification of oxidative stress, e.g. catalases and peroxidases, which require heme-iron for activity.

4. Conclusions

This study identified the first ferrireductase involved in RIA of a filamentous fungus. Moreover, this work demonstrated that copper-independent siderophore-mediated iron uptake increases resistance of *A. fumigatus* against copper shortage. In contrast, iron acquisition of siderophore-lacking fungal species such as *S. cerevisiae*, *C. albicans* and *C. neoformans* relies mainly on copper-dependent RIA. Inactivation of the siderophore system and, in particular, of both the siderophor system and FreB increased sensitivity to copper shortage also in *A. fumigatus* underlining the interconnection of these two metals. Previously, iron starvation was also found to impact zinc metabolism (Yasmin et al., 2009). Iron starvation downregulates various iron-dependent pathways to spare iron to prolong survival (Hortschansky et al., 2007; Schrettl et al., 2010). MR like FreB are heme-iron-dependent enzymes and therefore their upregulation during iron starvation demonstrates metabolic prioritization of available iron during this condition.

Acknowledgment

This work was supported by the Austrian Science Foundation Grant FWF P21643-B11.

Appendix A. Supplementary material

Supplementary data associated with this article can be found, in the online version, at doi:10.1016/j.fgb.2011.07.009.

References

Aguirre, J. et al., 2005. Reactive oxygen species and development in microbial eukaryotes. Trends Microbiol. 13, 111–118.

Altschul, S.F. et al., 1997. Gapped BLAST and PSI-BLAST: a new generation of protein database search programs. Nucleic Acids Res. 25, 3389–3402.

Baek, Y. et al., 2008. *Candida albicans* ferric reductases are differentially regulated in response to distinct forms of iron limitation by the Rim101 and CBF transcription factors. Eukaryot. Cell 7, 1168–1179.

Eichhorn, H. et al., 2006. A ferroxidation/permeation iron uptake system is required for virulence in *Ustilago maydis*. Plant Cell 18, 3332–3345.

Eisendle, M. et al., 2003. The siderophore system is essential for viability of *Aspergillus nidulans*: functional analysis of two genes encoding l-ornithine N 5-monooxygenase (sidA) and a non-ribosomal peptide synthetase (sidC). Mol. Microbiol. 49, 359–375.

Frey, R. et al., 2009. NADPH oxidase-dependent signaling in endothelial cells: role in physiology and pathophysiology. Antioxid. Redox Signal. 11, 791–810.

Galagan, J.E. et al., 2005. Sequencing of *Aspergillus nidulans* and comparative analysis with *A. fumigatus* and *A. oryzae*. Nature 438, 1105–1115.

Georgatsou, E. et al., 1997. The yeast Fre1p/Fre2p cupric reductases facilitate copper uptake and are regulated by the copper-modulated Mac1p activator. J. Biol. Chem. 272, 13786–13792.

Grissa, I. et al., 2010. The Nox/ferric reductase/ferric reductase-like families of Eumycetes. Fungal Biol. 114, 766–777.

Haas, H. et al., 2003. Characterization of the *Aspergillus nidulans* transporters for the siderophores enterobactin and triacetylfusarinine C. Biochem. J. 371, 505–513.

Haas, H. et al., 2008. Siderophores in fungal physiology and virulence. Annu. Rev. Phytopathol. 46, 149–187.

Halliwell, B., Gutteridge, J., 1984. Oxygen toxicity, oxygen radicals, transition metals and disease. Biochem. J. 219, 1–14.

Hammacott, J. et al., 2000. *Candida albicans* CFL1 encodes a functional ferric reductase activity that can rescue a *Saccharomyces cerevisiae* fre1 mutant. Microbiology 146, 869–876.

Hassett, R. et al., 1998. Spectral and kinetic properties of the Fet3 protein from *Saccharomyces cerevisiae*, a multinuclear copper ferroxidase enzyme. J. Biol. Chem. 274, 23274–23282.

Hortschansky, P. et al., 2007. Interaction of HapX with the CCAAT-binding complex – a novel mechanism of gene regulation by iron. EMBO J. 26, 3157–3168.

Ibrahim, A.S. et al., 2010. The high affinity iron permease is a key virulence factor required for *Rhizopus oryzae* pathogenesis. Mol. Microbiol. 77, 587–604.

Jung, W. et al., 2008. Iron source preference and regulation of iron uptake in *Cryptococcus neoformans*. PLoS Pathog. 4.

Knight, S. et al., 2002. Reductive iron uptake by *Candida albicans*: role of copper, iron and the TUP1 regulator. Microbiology 148, 29–40.

Knight, S.A. et al., 2005. Iron acquisition from transferrin by *Candida albicans* depends on the reductive pathway. Infect Immun. 73, 5482–5492.

Kosman, D., 2003. Molecular mechanisms of iron uptake in fungi. Mol. Microbiol. 47, 1185–1197.

Kosman, D.J., 2010. Redox cycling in iron uptake, efflux, and trafficking. J. Biol. Chem. 285, 26729–26735.

Kubodera, T. et al., 2000. Pyrithiamine resistance gene (ptrA) of *Aspergillus oryzae*: cloning, characterization and application as a dominant selectable marker for transformation. Biosci. Biotechnol. Biochem. 64, 1416–1421.

McDonagh, A. et al., 2008. Sub-telomere directed gene expression during initiation of invasive aspergillosis. PLoS Pathog. 4, e1000154.

Neron, B. et al., 2009. Mobyle: a new full web bioinformatics framework. Bioinformatics 25, 3005–3011.

Nielsen, M. et al., 2006. Efficient PCR-based gene targeting with a recyclable marker for *Aspergillus nidulans*. Fungal Genet. Biol. 43, 54.

Nierman, W.C. et al., 2005. Genomic sequence of the pathogenic and allergenic filamentous fungus *Aspergillus fumigatus*. Nature 438, 1151–1156.

Nyhus, K. et al., 1997. Ferric iron reduction by *Cryptococcus neoformans*. Infect Immun. 65, 434–438.

Oberegger, H. et al., 2001. SREA is involved in regulation of siderophore biosynthesis, utilization and uptake in *Aspergillus nidulans*. Mol. Microbiol. 41, 1077–1089.

Philpott, C., Protchenko, O., 2008. Response to iron deprivation in *Saccharomyces cerevisiae*. Eukaryot. Cell 7, 20–27.

Pontecorvo, G. et al., 1953. The genetics of *Aspergillus nidulans*. Adv. Genet. 5, 141–238.

Punt, P.J., van den Hondel, C.A., 1992. Transformation of filamentous fungi based on hygromycin B and phleomycin resistance markers. Methods Enzymol. 216, 447–457.

Ramanan, N., Wang, Y., 2000. A high-affinity iron permease essential for *Candida albicans* virulence. Science 288, 1062–1064.

Rees, E., Thiele, D., 2007. Identification of a vacuole-associated metalloreductase and its role in Ctr2-mediated intracellular copper mobilization. J. Biol. Chem. 282, 21629–21638.

Roman, D. et al., 1993. The fission yeast ferric reductase gene frp1+ is required for ferric iron uptake and encodes a protein that is homologous to the gp91-phox subunit of the human NADPH phagocyte oxidoreductase. Mol. Cell. Biol. 13, 4342–4350.

Sambrook, J. et al. (Eds.), 1992. Molecular Cloning – A Laboratory Manual. Cold Spring Habor, New York.

Schrettl, M. et al., 2004. Siderophore biosynthesis but not reductive iron assimilation is essential for *Aspergillus fumigatus* virulence. J. Exp. Med. 200, 1213–1219.

Schrettl, M. et al., 2007. Distinct roles for intra- and extracellular siderophores during *Aspergillus fumigatus* infection. PLoS Pathog. 3, 1195–1207.

Schrettl, M. et al., 2008. SreA-mediated iron regulation in *Aspergillus fumigatus*. Mol. Microbiol. 70, 27–43.

Schrettl, M. et al., 2010. HapX-mediated adaption to iron starvation is crucial for virulence of *Aspergillus fumigatus*. PLoS Pathog. 6 (9), pii:e1001124.

Singh, A. et al., 2007. The metalloreductase Fre6p in Fe-efflux from the yeast vacuole. J. Biol. Chem. 282, 28619–28626.

Sugareva, V. et al., 2006. Characterisation of the laccase-encoding gene abr2 of the dihydroxynaphthalene-like melanin gene cluster of *Aspergillus fumigatus*. Arch. Microbiol. 186, 345–355.

Tekaia, F., Latge, J.P., 2005. *Aspergillus fumigatus*: saprophyte or pathogen? Curr. Opin. Microbiol. 8, 385–392.

Wallner, A. et al., 2009. Ferricrocin, a siderophore involved in intra- and transcellular iron distribution in *Aspergillus fumigatus*. Appl. Environ. Microbiol. 75, 4194–4196.

Wang, H., Joseph, J.A., 1999. Quantifying cellular oxidative stress by dichlorofluorescein assay using microplate reader. Free Radical Biol. Med. 27, 612–616.

Yasmin, S. et al., 2009. The interplay between iron and zinc metabolism in *Aspergillus fumigatus*. Fungal Genet. Biol. 46, 707–713.